

AD-A120 430

COLLISION STUDIES ON MULTIPLY CHARGED IONS(U)  
CONNECTICUT UNIV STORRS DEPT OF PHYSICS E POLLACK  
OCT 82 ARO-18613. 2-PH DARG29-81-K-0141

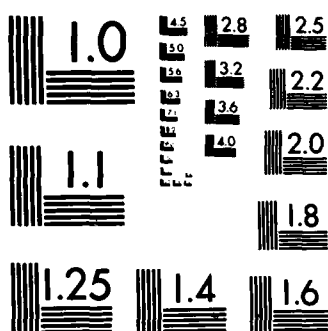
1/1

UNCLASSIFIED

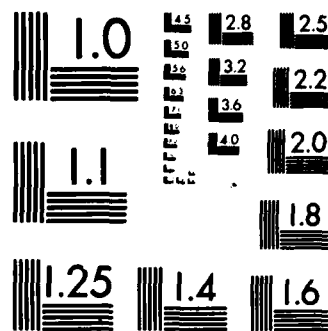
F/G 20/8

NL

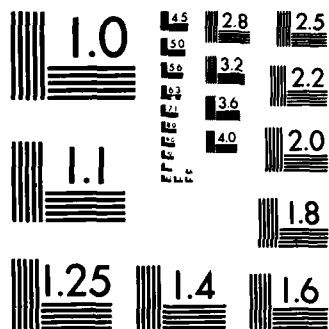




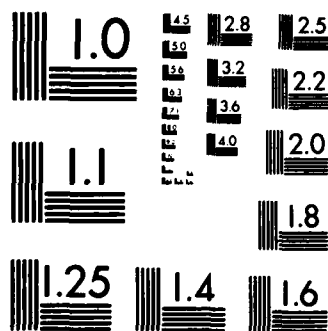
MICROCOPY RESOLUTION TEST CHART  
NATIONAL BUREAU OF STANDARDS-1963-A



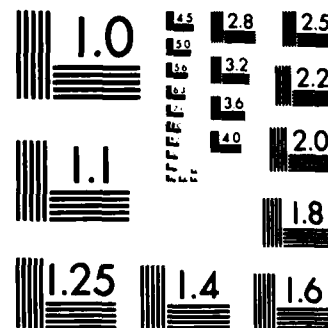
MICROCOPY RESOLUTION TEST CHART  
NATIONAL BUREAU OF STANDARDS-1963-A



MICROCOPY RESOLUTION TEST CHART  
NATIONAL BUREAU OF STANDARDS-1963-A



MICROCOPY RESOLUTION TEST CHART  
NATIONAL BUREAU OF STANDARDS-1963-A



MICROCOPY RESOLUTION TEST CHART  
NATIONAL BUREAU OF STANDARDS-1963-A

READ INSTRUCTIONS  
BEFORE COMPLETING FORM

AD A120430

Approved for public release; distribution unlimited.

# DTIC ELECTE

OCT 19 1982

**F**

The view, opinions, and/or findings contained in this report are those of the author(s) and should not be construed as an official Department of the Army position, policy, or decision, unless so designated by other documentation.

ions	excitation
free electrons	particle collisions
electron capture	argon
gas discharge	

Gaseous discharges contain ions in a number of charge states. Collisions between these ions and atoms in the discharge result in the production of excited ions and atoms as well as free electrons. Single electron capture collisions involving doubly charged ions with atoms are particularly important in determining the behavior of the discharge since they result in two ions with one generally in an excited state. Such collisions are not well understood. In this context we have studied electron capture in  $\text{Ar}^{2+} + \text{Ar}$  because of the importance of argon.

20. ABSTRACT CONTINUED

as a discharge gas and because there were substantial difficulties in understanding single electron capture processes in the collision. Prior to this work, and as late as July 1982, published results on single electron capture in  $\text{Ar}^{2+} + \text{Ar}$  identified the dominant channels as  $\text{Ar}^+(^2P) + \text{Ar}^+(^2P)$  and  $\text{Ar}^+(^2P) + \text{Ar}^+(3s3p)$ . Capture to  $\text{Ar}^+(3s3p)$  was particularly difficult to understand and raised fundamental questions about the underlying theory. We have shown however that the final states are of the type  $\text{Ar}^+(^2P) + \text{Ar}^+(3s^2 3p^4 n\ell)$  with  $n\ell$  being predominantly 3d and 4p at low keV energies. Our laboratory has measured the cross sections for the important final channels in the single electron capture collisions as well as for the direct scattering and for the double electron capture cases. It is particularly interesting that the direct scattering does not occur with Ar target excitation as was found in  $\text{Ar}^{2+} + \text{Ar}$ . We have also shown that long lived highly excited states of  $\text{Ar}^{2+}$  make important contributions to the charge exchange. We interpret our results and propose a simple model of the collision.



Accession For	
NTIS GRA&I	<input checked="" type="checkbox"/>
DTIC TAB	<input type="checkbox"/>
Unannounced	<input type="checkbox"/>
Justification	
By _____	
Distribution/	
Availability Codes	
Dist	Avail and/or Special
A	

Unclassified

Final Report: Collision Studies on Multiply Charged Ions  
Grant DAAG29-81-K-0141

Submitted by: Dr. Edward Pollack  
Physics Department  
The University of Connecticut  
Storrs, Connecticut 06268  
27 September 1982

### Abstract

Gaseous discharges contain ions in a number of charge states. Collisions between these ions and atoms in the discharge result in the production of excited ions and atoms as well as free electrons. Single electron capture collisions involving doubly charged ions with atoms are particularly important in determining the behavior of the discharge since they result in two ions with one generally in an excited state. Such collisions are not well understood. In this context we have studied electron capture in  $\text{Ar}^{2+} + \text{Ar}$  because of the importance of argon as a discharge gas and because there were substantial difficulties in understanding single electron capture processes in the collision.

Prior to this work, and as late as July 1982, published results on single electron capture in  $\text{Ar}^{2+} + \text{Ar}$  identified the dominant channels as  $\text{Ar}^+(^2\text{P}) + \text{Ar}^+(^2\text{P})$  and  $\text{Ar}^+(^2\text{P}) + \text{Ar}^+(3s3p^6)$ . Capture to  $\text{Ar}^+(3s3p^6)$  was particularly difficult to understand and raised fundamental questions about the underlying theory. We have shown however that the final states are of the type  $\text{Ar}^+(^2\text{P}) + \text{Ar}^+(3s^23p^4n\ell)$  with  $n\ell$  being predominantly 3d and 4p at low keV energies. Our laboratory has measured the cross sections for the important final channels in the single electron capture collisions as well as for the direct scattering and for the double electron capture cases. It is particularly interesting that the direct scattering does not occur with Ar target excitation as was found in  $\text{Ar}^+ + \text{Ar}$ . We have also shown that long lived highly excited states of  $\text{Ar}^{2+}$  make important contributions to the charge exchange. We interpret our results and propose a simple model of the collision.

### Introduction

There is currently a substantial effort being devoted to studying charge-exchange in ion-atom collisions. This is due in large part to the importance of charge-exchange collisions in gaseous discharges and to the challenges presented to the theory by the electron rearrangement. Exchange processes involving singly charged ions and atoms have been investigated in detail both experimentally and theoretically for a number of years and are now reasonably well understood. Electron capture processes involving doubly (and multiply) charged ions are not yet well understood.

A single electron capture collision between a doubly charged ion and an atom yields two ions with one generally in an excited state. Single electron capture in  $\text{Ar}^{2+} + \text{Ar}$  is of particular interest at this time since it has been studied for a number of years and there are still substantial difficulties in understanding the collision. Electron capture in  $\text{Ar}^{2+} + \text{Ar}$  is discussed in References 1-7 where citations to the earlier literature are given. Two recent studies of this collision<sup>2,3</sup> conclude that the dominant single electron capture processes result in  $\text{Ar}^+(^2\text{P}) + \text{Ar}^+(3s3p^6)$  and  $\text{Ar}^+(^2\text{P}) + \text{Ar}^+(^2\text{P})$  final states. The  $\text{Ar}^+(^2\text{P}) + \text{Ar}^+(3s3p^6)$  channel (ground state + first excited state) is particularly difficult to justify<sup>1</sup> since it is excited via a two electron process. These recently reported experimental studies were made at energies in the range<sup>2</sup> 554 to 1446 eV and at 540 eV.<sup>3</sup> We report results<sup>8</sup> at somewhat higher energies and conclude that the dominant small angle processes are of the type  $\text{Ar}^{2+}(^3\text{P}) + \text{Ar} \rightarrow \text{Ar}^+(^2\text{P}) + \text{Ar}^+(3s^2 3p^4 nl)$  with  $nl$  primarily being  $3d$  and  $4p$ .

It is useful to understand the single electron capture processes in  $\text{Ar}^{2+} + \text{Ar}$  since the basic problems in the Argon Case are characteristic of those associated with collisions involving multiply charged ions with atoms. In the

general collision of this type there are various final charge and excited state configurations that lie close in energy. Before such collisions can be well understood it is essential to resolve questions involving the relative importance of the two vs. one electron process in single electron capture, the applicability of spin conservation, the relative importance of exothermic channels, and the role of excited projectile states.

Single electron capture in  $\text{Ar}^{2+} + \text{Ar}$  is studied at low keV energies and for scattering angles out to one degree to address the above problems. We justify the assignment of  $\text{Ar}^+(^2\text{P}) + \text{Ar}^+(3s^2 3p^4 n l)$  as the important final states and present differential cross-sections for the dominant processes. Our studies show contributions to the scattering from highly excited and long lived final states in the beam as expected.<sup>1,9</sup> In addition we present results for the direct scattering and for the double electron capture collisions. We find that the direct  $\text{Ar}^{2+} + \text{Ar}$  collision shows no Ar excitation in the  $\tau = E\theta$  (reduced scattering angle = beam energy x scattering angle) range studied. This is particularly interesting since the  $\text{Ar}^+ + \text{Ar}$  collision resulted in excitation of Ar(4s and 4p) in the same  $\tau$  range.<sup>10</sup>

### Experimental Technique

The basic experimental techniques have been discussed in earlier papers<sup>11-14</sup> and are only briefly summarized here. A mass analyzed and well collimated  $\text{Ar}^{2+}$  beam is directed into a scattering cell containing the Ar target gas. The beam scatters under single collision conditions into a detector chamber which rotates about a point in the scattering cell. The scattered ions are then energy analyzed using a parallel plate electrostatic energy analyzer. The neutral component, resulting from double electron capture collisions, passes through the analyzer to a detector positioned beyond it.

In  $\text{Ar}^{2+} + \text{Ar} \rightarrow \text{Ar}^+ + \text{Ar}^+$  the final states are identified using  $\Delta E$ , the measured kinetic energy loss or gain of the scattered  $\text{Ar}^+$ . Since the  $\text{Ar}^+$  energy spectra have no reference peak from which the  $\Delta E$  can be determined, it is necessary to measure both the incident  $\text{Ar}^{2+}$  and scattered  $\text{Ar}^+$  beam energies and use the known electrostatic energy analyzer constant to find  $\Delta E$ . This requires the analyzer voltage to be increased by about a factor of 2 in switching between the incident  $\text{Ar}^{2+}$  and the scattered  $\text{Ar}^+$  beams. In addition to this problem, contact potentials in the electrostatic energy analyzer circuit lead to uncertainties in assigning the energy at the peaks of the  $\text{Ar}^+$  spectra. Because of the change in charge state, the presence of contact potentials in the scattering cell as well can result in additional errors of about one eV in the measured  $\Delta E$  values. In the present work the above problems are resolved by using  $\text{Ar}^{2+} + \text{He} \rightarrow \text{Ar}^+ + \text{He}^+$  collisions as an energy reference. In this case the possible final states are far apart in  $\Delta E$ .<sup>15</sup> Figure 1 shows composite spectra (peaks A and B) for  $\text{Ar}^{2+} + \text{Ar} \rightarrow \text{Ar}^+ + \text{Ar}^+$  at an energy  $E = 2.9$  keV and laboratory scattering angle  $\theta = 0.15$  deg, and a reference (peak R) from  $\text{Ar}^{2+} + \text{He} \rightarrow \text{Ar}^+ + \text{He}^+$  at  $E = 2.9$  keV,  $\theta = 0$



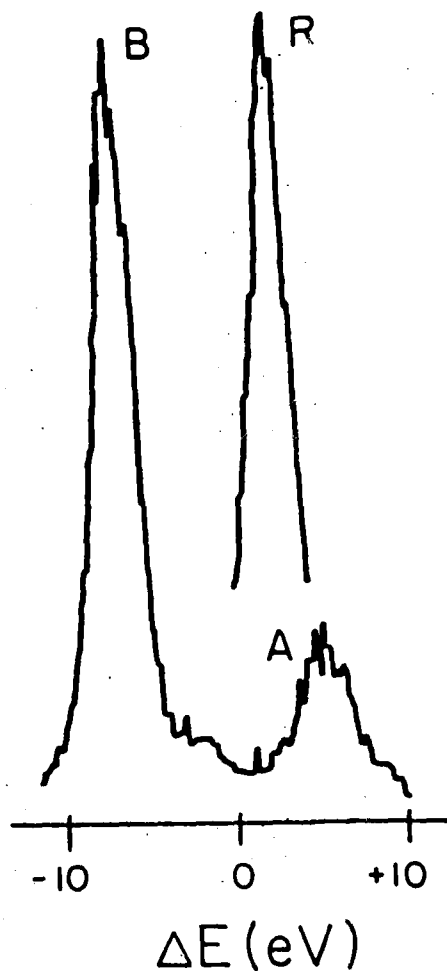


Figure 1. Composite spectra showing  $E = 2.9$  keV  $\text{Ar}^+ + \text{Ar} \rightarrow \text{Ar}^+ + \text{Ar}^+$  (A and B) at  $0.15$  deg. and  $\text{Ar}^+ + \text{He} \rightarrow \text{Ar}^+ + \text{He}^+$  (R) at  $0$  deg. Peak R serves as an energy reference and corresponds to  $\text{Ar}^{2+}(3p) + \text{He} \rightarrow \text{Ar}^+(2p) + \text{He}^+(^2S)$ :  $Q = 3$  eV. Peak B at this angle has its maximum at  $Q = -6.4$  eV and is attributed to  $\text{Ar}^+(2p) + \text{Ar}^+(3s^23p^43d)$ . At all angles this peak is due to final  $\text{Ar}^+(2p) + \text{Ar}^+(3s^23p^4nl)$  states. Peak A has a  $Q \approx 5.6$  eV and moves toward the right, corresponding to larger positive  $Q$  values, with increasing scattering angle.

deg. The reference peak is assigned to  $\text{Ar}^{2+}(^3\text{P}) + \text{He} \rightarrow \text{Ar}^+(^2\text{P}) + \text{He}^+(^2\text{S})$  with  $\Delta E = 3$  eV (agreeing to within one eV with the value computed using the known analyzer constant). The reference peak is obtained at 0 deg to avoid having to make a correction for the kinematically required energy loss at non-zero scattering angles. Using peak R as a reference, peak B in Figure 1 has a Q value (the endothermic or exothermic energy =  $\Delta E - E\theta^2$  at small angles<sup>13</sup>) at the peak maximum of  $-6.4 \pm 0.25$  eV. At the scattering angle shown in Figure 1 this energy loss corresponds to  $\text{Ar}^{2+}(^3\text{P}) + \text{Ar} \rightarrow \text{Ar}^+(^2\text{P}) + \text{Ar}^+(3s^2 3p^4 3d)$ . At larger angles peak B shows structure attributed to the presence of a second state ( $Q = -7.4 \pm 0.25$  eV) and to weaker contributions from higher excited states. Peak A in Figure 1 is due to an exothermic process with  $Q \approx +5.6$  eV at this scattering angle ( $Q$  at the maximum of the spectrum is found to depend on  $\theta$ ).

Figure 2 is an energy spectrum of  $\text{Ar}^+$  at  $E = 2.9$  keV,  $\theta = 1$  deg. for  $\Delta E$  in a range to +28 eV. The figure shows structure at energies corresponding to  $\text{Ar}^{2+}(^3\text{P}$  and  $^1\text{D}) + \text{Ar} \rightarrow \text{Ar}^+(^2\text{P}) + \text{Ar}^+(^2\text{P})$  but stronger contributions from other states are clearly present. Highly excited states of  $\text{Ar}^{2+}$  are responsible for the additional features in the spectrum. Electron capture to ground state  $\text{Ar}^+(^2\text{P}) + \text{Ar}^+(^2\text{P})$  from  $\text{Ar}^{2+}(^3\text{P})$ , ( $^1\text{D}$ ), and ( $^1\text{S}$ ) would result in Q values of +11.8, +13.6, and +16 eV respectively (all exothermic). Capture to  $\text{Ar}^+(^2\text{P}) + \text{Ar}^+(3s3p^6, ^2\text{S})$  (the lowest lying excited configuration) from these initial states would give rise to Q values of -1.6, +0.1, and +2.5 eV respectively. The measured Q of +5.6 eV in Figure 1 cannot be explained by an  $\text{Ar}^{2+}$  beam in any of the three generally expected states. We attribute peak A at this angle to highly excited states such as  $\text{Ar}^{2+}(^1\text{P}^0)$  and ( $^5\text{D}^0$ ) lying about 18 eV above the ground state<sup>15</sup> and which are expected to be long lived.

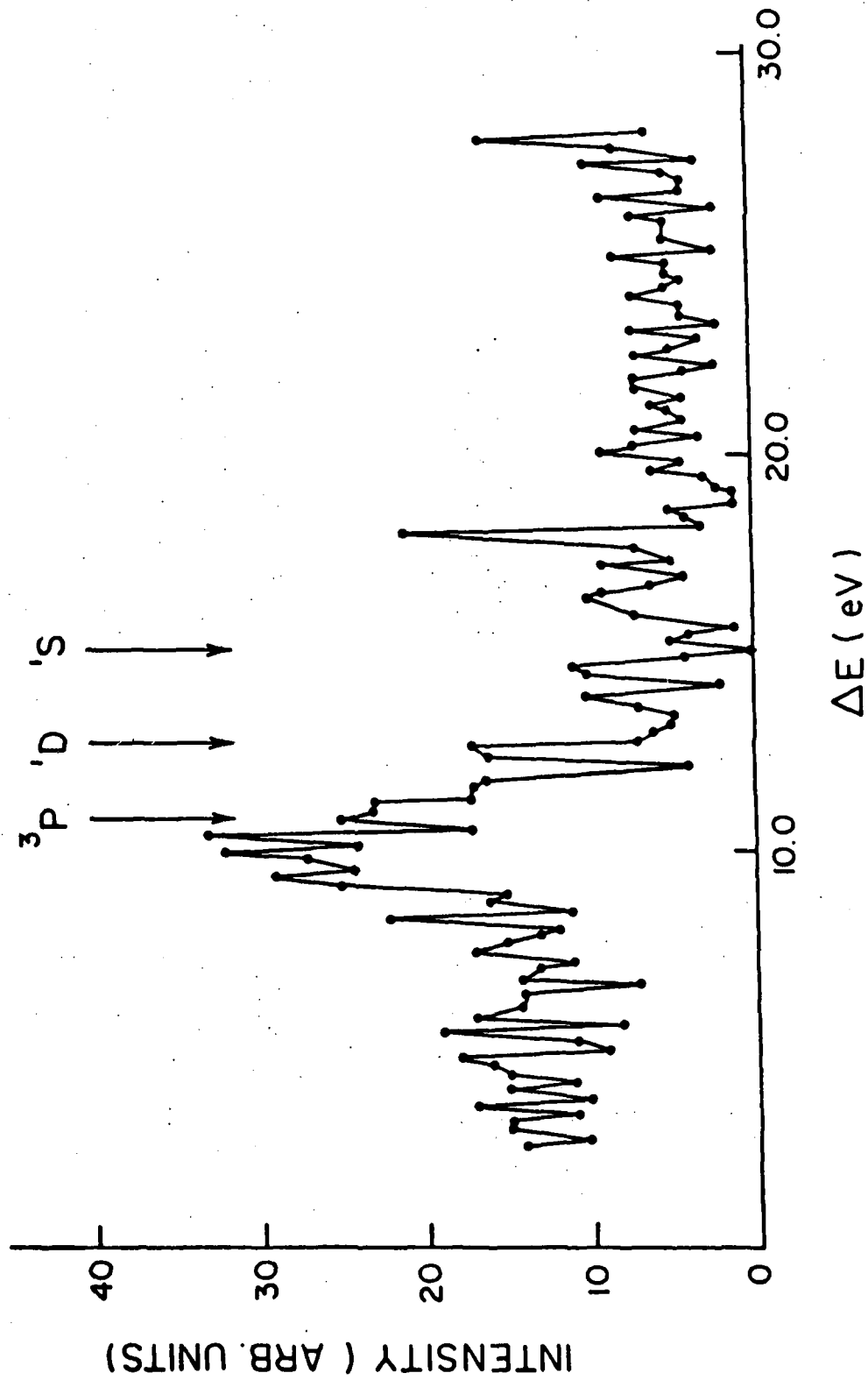


Figure 2. Energy spectrum for the exothermic channels in  $E = 2.9 \text{ keV}$ ,  $\theta = 1.0 \text{ deg}$ .  $\text{Ar}^{2+} + \text{Ar} \rightarrow \text{Ar}^{+} + \text{Ar}^{+}$  collisions. The peak shows important structure near  $\Delta E = 10 \text{ eV}$  in comparison to  $\Delta E = 5.6 \text{ eV}$  at  $\theta = 0.15 \text{ deg}$  in Figure 1. The arrows are at positions, corrected for the kinematic energy loss, corresponding to  $\text{Ar}^{2+}(3P)$ ,  $(1D)$ , and  $1(S) + \text{Ar} \rightarrow \text{Ar}^{+}(2P) + \text{Ar}^{+}(2P)$ . The

### Experimental Results and Interpretations

The single electron capture in  $\text{Ar}^{2+} + \text{Ar}$  is found to involve both endothermic processes (B) and weaker exothermic processes (A). Figure 3 shows  $\rho \approx \theta^2 \sigma(\theta)$  (the reduced cross section =  $\theta^2 \times$  the differential cross section) at energies of 2.4, 2.9, and 3.5 keV for peak B corresponding to  $\text{Ar}^{2+}(^3\text{P}) + \text{Ar} \rightarrow \text{Ar}^+(^2\text{P}) + \text{Ar}^+(3s^2 3p^4 nl)$ . Measurements made at other energies in the range shown are found to be in agreement with the results in Figure 3 but are not plotted. For the  $\tau$  range studied the dominant processes in B correspond to those with  $|Q| \geq 6.4$  eV and are consistent only with final  $\text{Ar}^+(^2\text{P}) + \text{Ar}^+(3s^2 3p^4 nl)$  states. The behavior of the  $\rho$  vs.  $\tau$  plot suggests that the electron capture occurs via curve crossing mechanisms.<sup>14</sup>

A detailed study of peak B is made at  $E = 2.4$  keV. At small angles the single electron capture channels primarily result in two final state configurations (the spectra do however show evidence of small contributions from additional states). The following assumptions are made in identifying the final states: (1) The collision involves the capture of a single electron from the Ar by the  $\text{Ar}^{2+}$  which provides an unchanged core for the final  $\text{Ar}^+$  state. (2) The Wigner spin rule applies.<sup>1</sup> Using the known ionization potentials and energy levels<sup>15</sup> the dominant single electron capture processes for the measured  $Q$  values of  $-6.4$  and  $-7.4 \pm 0.25$  eV are consistent with  $\text{Ar}^{2+}(^3\text{P}) + \text{Ar} \rightarrow \text{Ar}^+(^2\text{P}) + \text{Ar}^+(3s^2 3p^4 3d)$  and  $\text{Ar}^+(^2\text{P}) + \text{Ar}^+(3s^2 3p^4 4p)$ . Figure 4 shows  $\rho$  vs.  $\tau$  plots for the two dominant final channels. The similar envelope of these curves suggests that the two final channels are excited by a common primary interaction. The structure of the curves shows phase differences possibly due to branching at larger internuclear separation.

The direct scattering,  $\text{Ar}^{2+} + \text{Ar} \rightarrow \text{Ar}^{2+} + \text{Ar}$ , does not result in Ar excitation in the  $\tau$  range studied. This is unlike the case in  $\text{Ar}^+ + \text{Ar}$  where target excitation to 4s and 4p was found in this  $\tau$  range.<sup>10</sup> The reduced cross section

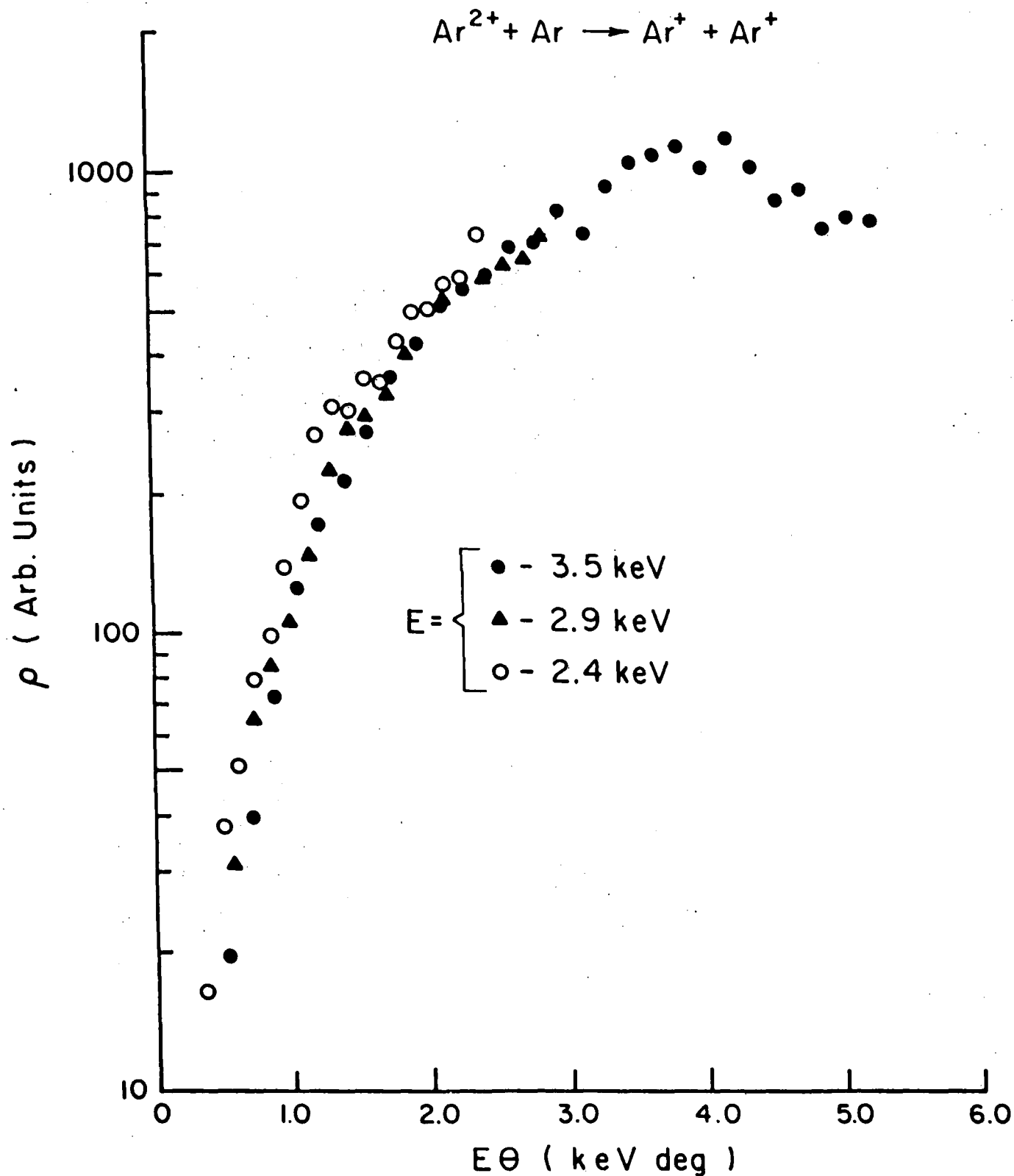


Figure 3. The reduced cross section for  $\text{Ar}^{2+}(^3\text{P}) + \text{Ar} \rightarrow \text{Ar}^+(^2\text{P}) + \text{Ar}^+(3s^2 3p^4 n1)$  at energies of 2.4, 2.9, and 3.5 keV. These are found to be the important single electron capture processes in the  $\tau$  range studied.

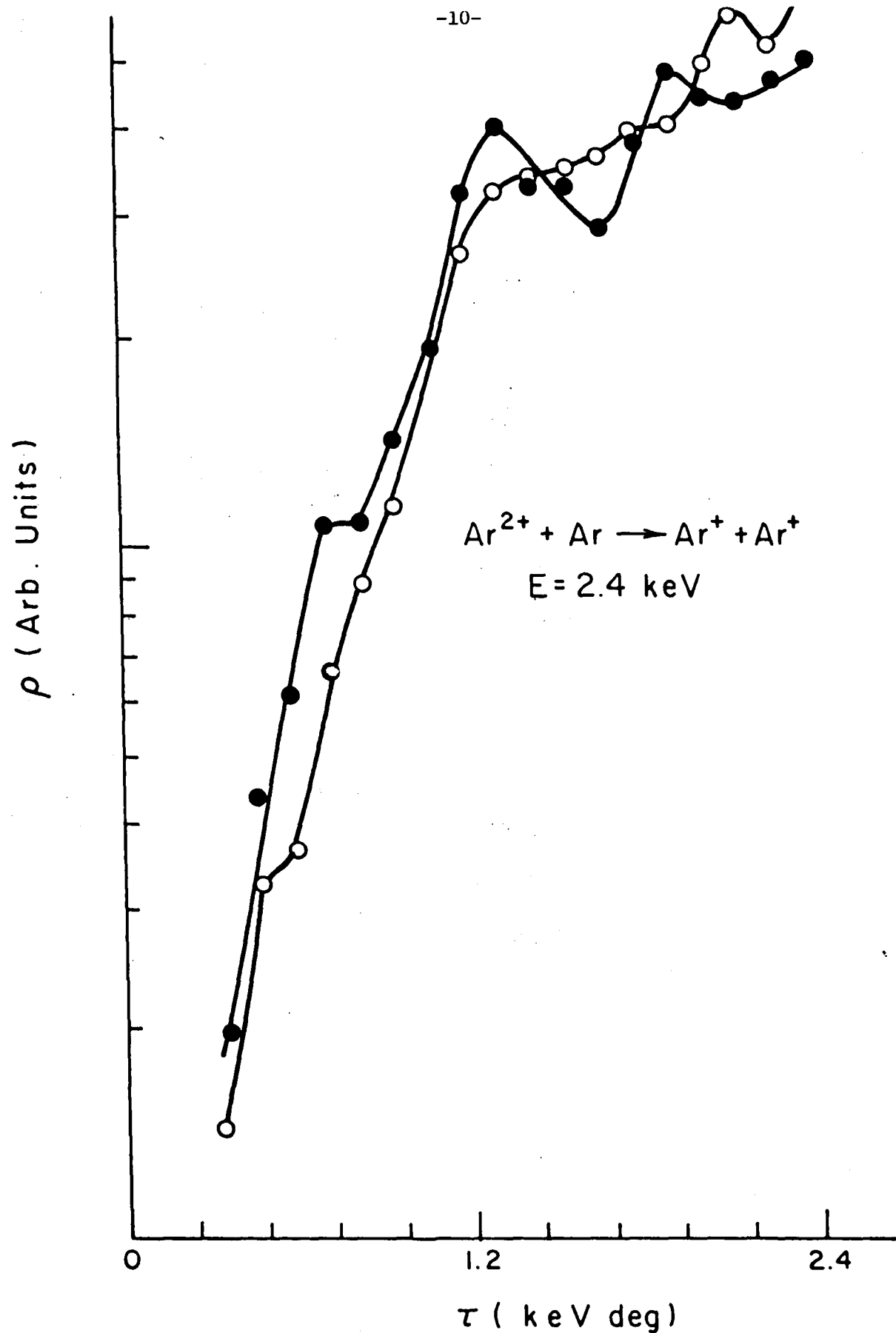


Figure 4. The reduced cross sections at  $E = 2.4 \text{ keV}$  for the dominant processes in the single electron capture collisions. The endothermic processes primarily are due to  $\bullet \text{Ar}^{2+}(3p) + \text{Ar} \rightarrow \text{Ar}^+ + \text{Ar}^+(3s^2 3p^4 3d)$  and  $\bullet \text{Ar}^{2+}(3p) + \text{Ar} \rightarrow \text{Ar}^+ + \text{Ar}^+(3s^2 3p^4 4p)$  in the  $\tau$  range shown.

for the direct scattering is shown in Figure 5 at energies of 2.4 and 3.4 keV. The  $\rho$  vs.  $\theta$  plots show approximately similar structure including maxima at common  $\theta$  values of 0.1, 0.4, 0.55, and 0.75 deg. This behavior is expected when resonant charge exchange channels are available.<sup>16,17</sup> Figure 6 shows the cross sections for the direct scattering and for the double electron capture collisions. The phase differences between the two cross sections are clearly seen showing that the major losses from the direct scattering (in this  $\theta$  range) are due to double electron capture collisions.

The behavior of the exothermic collisions is seen by comparing Figures 1 and 2. At  $\theta = 0.15$  deg the maximum is at a  $Q = 5.6$  eV and at  $\theta = 1$  deg it is near 10 eV. The region of maximum intensity is displaced to larger  $Q$  with increasing  $\theta$ . Figure 7 shows  $\rho$  vs.  $\tau$  plots for three processes corresponding to  $Q$  values of (a) +5.6 eV, (b) +10.4 eV, and (c) +11.6 eV. Within experimental error (c) is attributed to  $\text{Ar}^{2+}(^3\text{P}) + \text{Ar} \rightarrow \text{Ar}^{+}(^2\text{P}) + \text{Ar}^{+}(^2\text{P})$ . Processes a and b require the presence of highly excited  $\text{Ar}^{2+}$  states. The exothermic processes in this study are weaker than the endothermic ones (at  $E = 2.9$  keV,  $\theta = 1$  deg they differ by an order of magnitude).

Electron capture resulting in  $\text{Ar}^{+}(^2\text{P}) + \text{Ar}^{+}(3s^2 3p^4 n1)$  configurations in small angle  $\text{Ar}^{2+} + \text{Ar}$  collisions is not easily explained. In this collision the incident channel is weakly attractive, and the final channels are repulsive at large internuclear separation. Since the process is endothermic the incident and final potential energy curves do not cross (at large internuclear separation). As a starting point in our understanding of the collision we propose a simple model where the final states can be populated via couplings with a strongly attractive intermediate state, such as one associated with  $\text{Ar}^{2+} + \text{Ar}^*$ , which crosses the incident and final channels.<sup>8</sup> Figure 8 shows several potential energy curves for

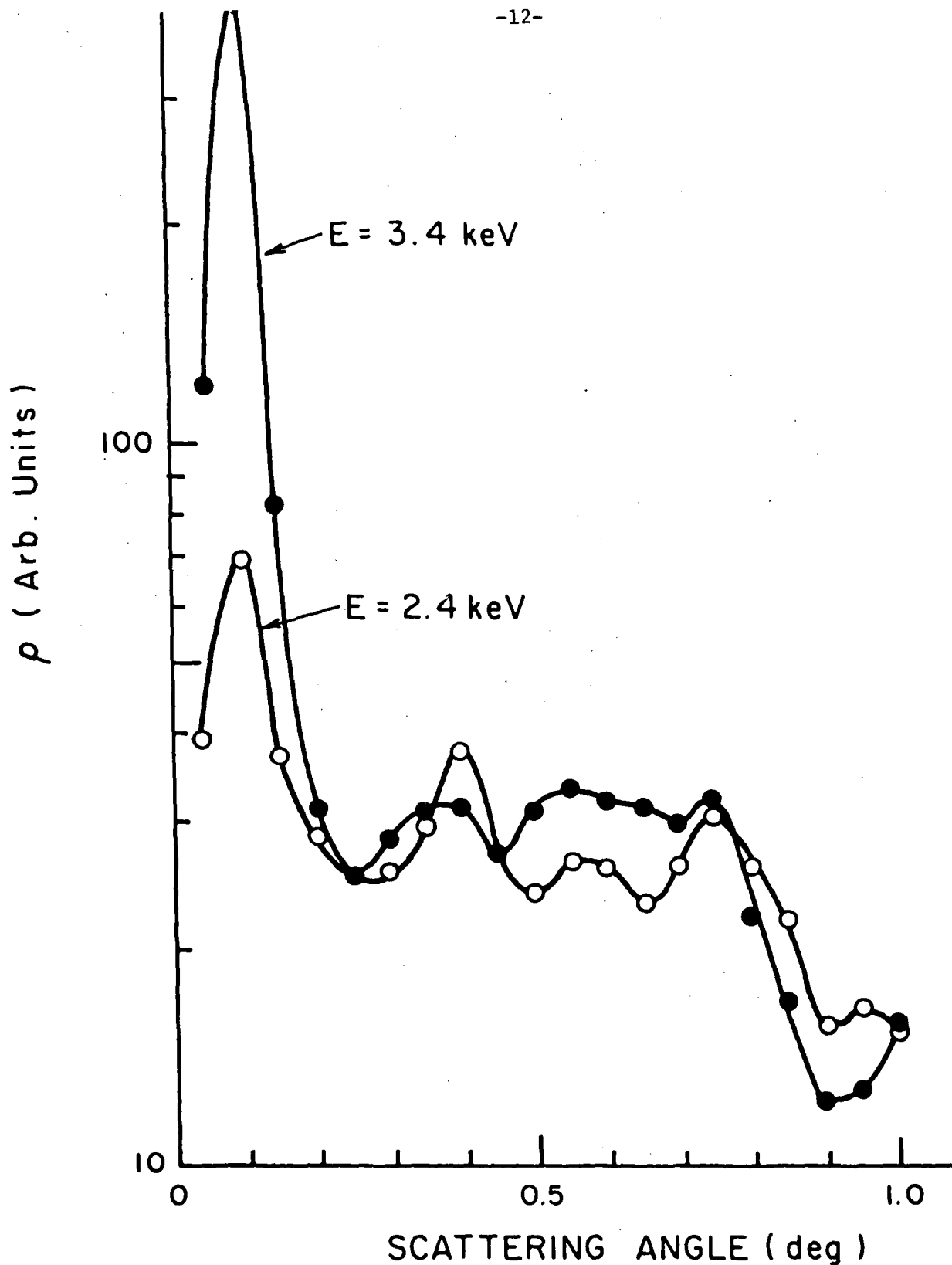


Figure 5. The reduced cross sections as a function of scattering angle for the direct scattering,  $\text{Ar}^{2+} + \text{Ar} \rightarrow \text{Ar}^{2+} + \text{Ar}$ , at energies at 2.4 and 3.4 keV. No target excitation is seen in the angular range studied and the structure at these angles is due to losses to the electron capture channels.



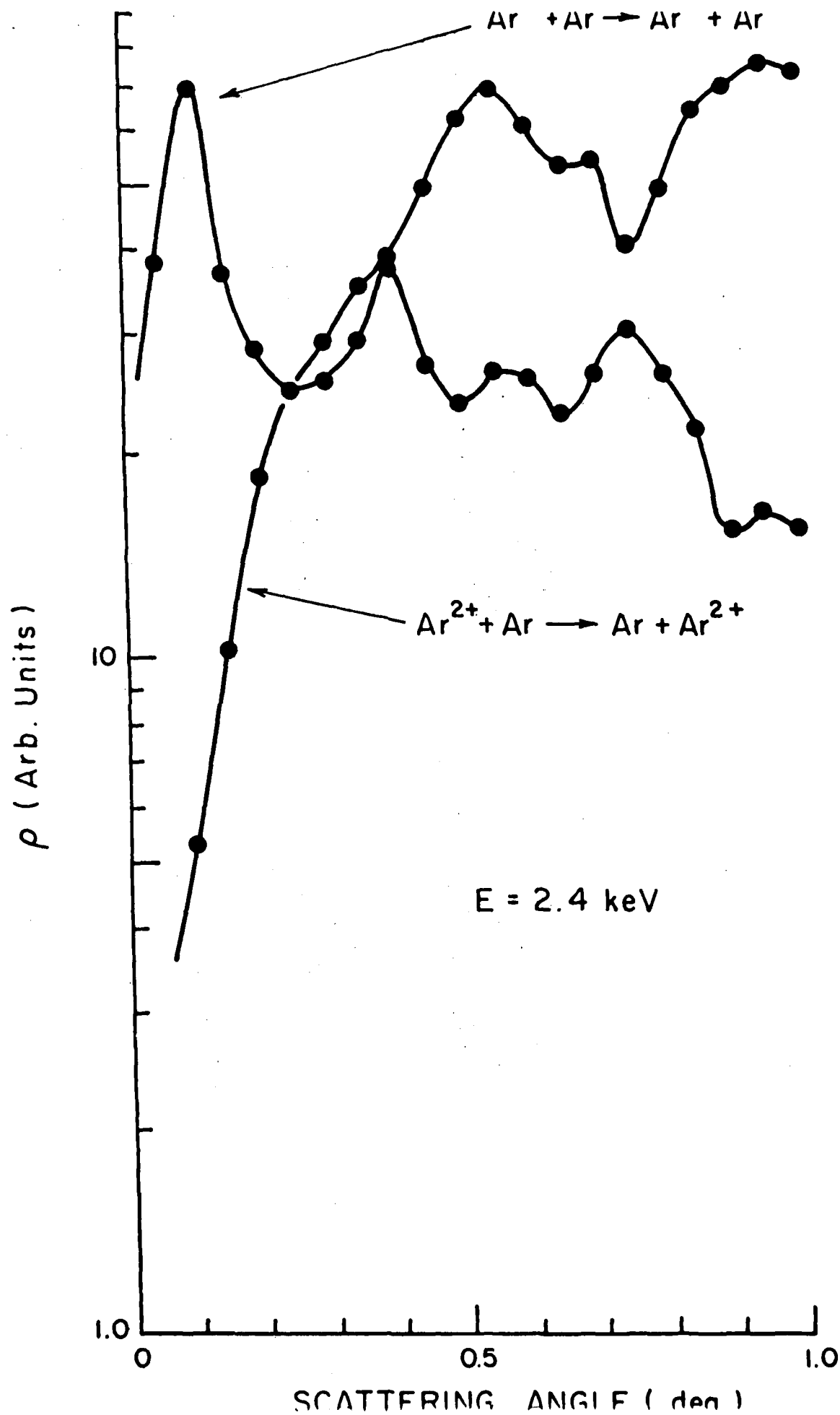


Figure 6. The reduced cross sections for the direct scattering and double electron capture collisions at  $E = 2.4 \text{ keV}$ . The cross sections are seen to be

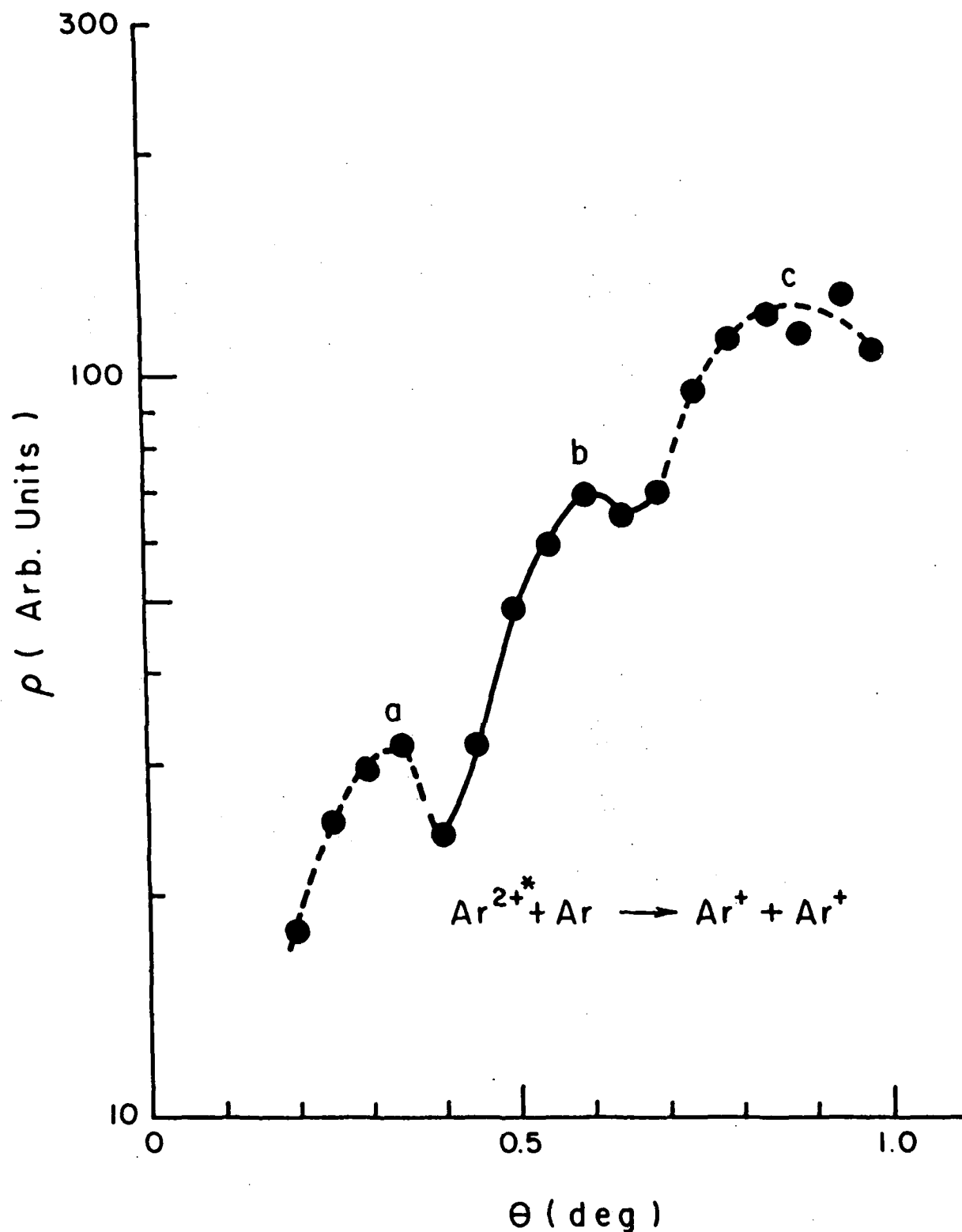


Figure 7. The reduced cross sections for the important processes contributing to the exothermic single electron capture channels. The peaks labelled a, b, and c correspond to processes having  $Q$  values of about 5.6, 10.4, and 11.6 eV respectively. Within experimental error (c) corresponds to  $\text{Ar}^{2+}(3p) + \text{Ar} \rightarrow \text{Ar}^+(2p) + \text{Ar}^+(2p)$ . Processes a and b are due to highly excited states in the incident  $\text{Ar}^{2+}$  beam.

the  $\text{Ar}^{2+} + \text{Ar}$  and  $\text{Ar}^+ + \text{Ar}^+$  systems. The curves for  $\text{Ar}^{2+} + \text{Ar}$  are plotted using a potential energy  $V(r) = -2\alpha e^2/r^4$  where  $\alpha$  is the polarizability of Ar ( $1.64 \times 10^{-24} \text{ cm}^3$ ),<sup>18</sup>  $e$  is the electronic charge, and  $r$  is the internuclear separation. The curve for  $\text{Ar}^{2+}(^3\text{P}) + \text{Ar}^*$  is plotted for  $\text{Ar}^*(4s)$  with  $\alpha = 48 \times 10^{-24} \text{ cm}^3$ <sup>19</sup> and is displaced at infinite separation by 11.5 eV above the  $\text{Ar}^{2+}(^3\text{P}) + \text{Ar}$ . Curves corresponding to several  $\text{Ar}^+ + \text{Ar}^+$  states are plotted using a Coulomb potential. Within the proposed simple model, excitation of  $\text{Ar}^+ + \text{Ar}^+(3s^2 3p^4 nl)$  involves a two step process: (1) An initial crossing between the incident  $\text{Ar}^{2+}(^3\text{P}) + \text{Ar}$  potential energy curve and one corresponding to a state such as  $\text{Ar}^{2+}(^3\text{P}) + \text{Ar}^*$  and (2) A transition (occurring near  $r = 4.5 \text{ \AA}$ ) from this intermediate state to  $\text{Ar}^+ + \text{Ar}^+(3s^2 3p^4 nl)$ . The behavior of the reduced cross section for peak B (Figure 4) is consistent with excitation of final states following a single primary interaction. In addition the peaking of  $\rho$  at small angles is expected from a potential that has both attractive and repulsive sections.<sup>14</sup> The  $\text{Ar}^{2+} + \text{Ar}^*$  is depopulated by crossings with the  $\text{Ar}^+ + \text{Ar}^+(3s^2 3p^4 nl)$  states, and the direct inelastic scattering should be weak (as found). Although the intermediate state also crosses  $\text{Ar}^+ + \text{Ar}^+(3s 3p^6)$ , this channel should only be weakly excited since it involves a two electron transition at the crossing.

The Q values found for peak A are not consistent with its excitation from only the  $^3\text{P}$ ,  $^1\text{D}$ , and  $^1\text{S}$  components of an  $\text{Ar}^{2+}$  beam. The peak can be explained by referring to Figure 8. One incident state contributing to the peak is assumed to lie about 18 eV above the ground state,  $\text{Ar}^{2+}(^3\text{P}) + \text{Ar}$ , at infinite separation. The potential energy curve for the state is essentially parallel to that of the ground state and it crosses potential energy curves of highly excited final states of  $\text{Ar}^+ + \text{Ar}^{+*}$  such as shown. Only one crossing is required for the single electron capture. For a given incident state, as the distance of closest approach

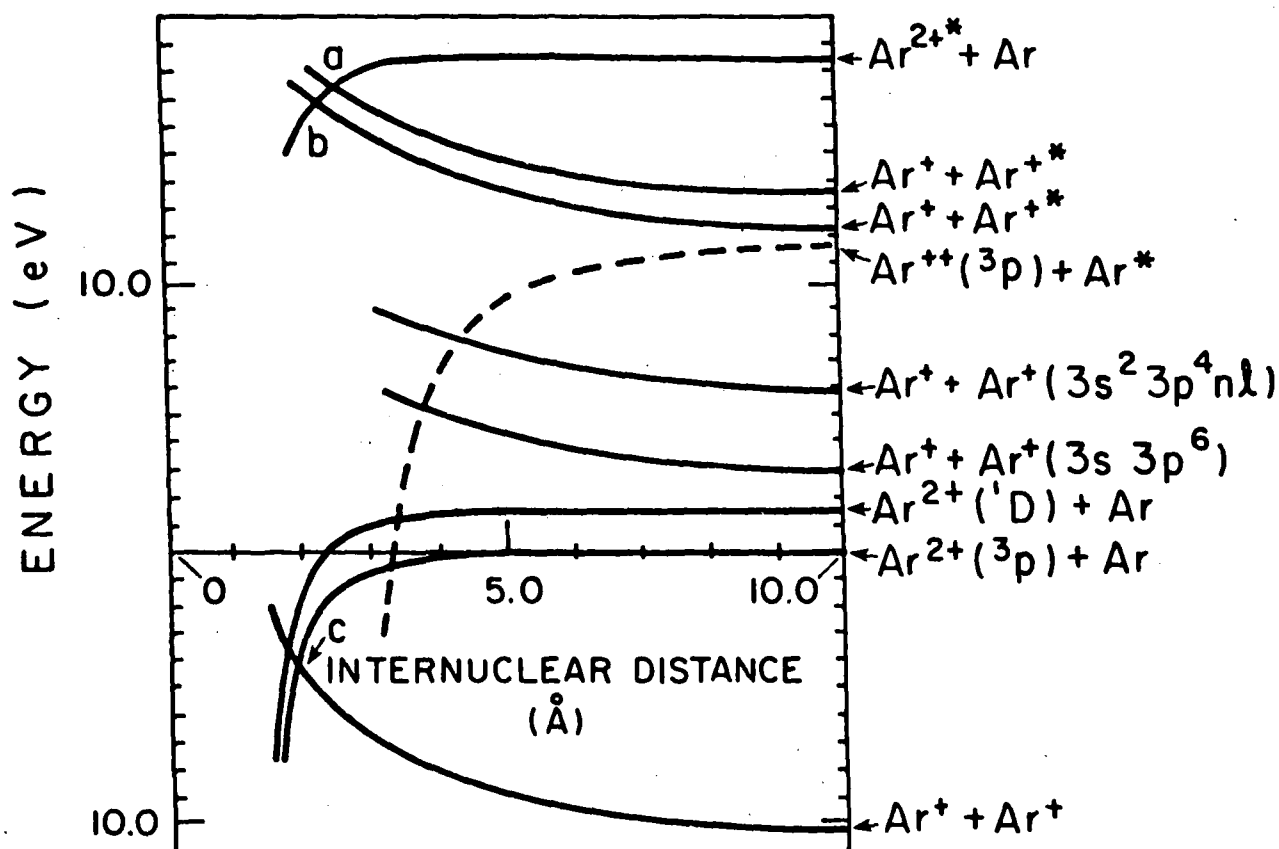


Figure 8. Potential energy curves for selected states in  $\text{Ar}^{2+} + \text{Ar}$  and  $\text{Ar}^+ + \text{Ar}^+$ . These simplified potential energy curves assume only a long range ion-atom interaction and a Coulomb repulsion to illustrate a model of the collision. The spacing between states at infinite separation is obtained from Ref. 15.  $\text{Ar}^{2+}(3p) + \text{Ar}^*$  corresponds to  $\text{Ar}^*(4s)$ . The  $\text{Ar}^+ + \text{Ar}^+(3s^2 3p^4 nl)$  is plotted for the lowest level which lies 16.4 eV above the  $\text{Ar}^+ + \text{Ar}^+$  ground state. All other states corresponding to  $nl$  configurations lie above it.  $\text{Ar}^{2+}(3p) + \text{Ar} \rightarrow \text{Ar}^+ + \text{Ar}^+(3s^2 3p^4 nl)$  can be populated at small angles by a process resulting from an initial transition to  $\text{Ar}^{2+}(3p) + \text{Ar}^*$  near  $r = 3\text{\AA}$  followed by a transition from this intermediate state to  $\text{Ar}^+ + \text{Ar}^+(nl)$  near  $r = 4.5\text{\AA}$ . Since the intermediate state crosses a large number of  $\text{Ar}^+ + \text{Ar}^+(nl)$  curves the direct inelastic scattering is weak. Excitation of  $\text{Ar}^+(3s 3p^6)$  is weak since it involves a two electron transition. Exothermic processes are due to interactions near points a, b, and c.

in the collision decreases, the scattering angle increases and the crossings populate lower lying final states. This results in an increase in Q value with increasing scattering angle and is in agreement with the experimental findings. The single crossing between the incident  $\text{Ar}^{2+}(^3\text{P}) + \text{Ar}$  curve and the final ground state curve results in (c).

The suggested collision model accounts for the important features of the single electron capture collisions and serves as a starting point in a rigorous theoretical treatment of the argon and similar problems. A careful analysis of the collision problem requires a detailed knowledge of the potential energy curves near the level crossings of interest and of the strength of the couplings between the states. Theoretical work<sup>20</sup> is underway to analyze the present results, by not only estimating the total cross section but also calculating the angular distribution of the final products involving different excited states. It should provide additional tests of the proposed reaction model.

### Conclusions

This study resolves several problems previously associated with single electron capture in low keV energy  $\text{Ar}^{2+} + \text{Ar}$  collisions. The dominant processes are found to be of the type  $\text{Ar}^{2+}(^3\text{P}) + \text{Ar} \rightarrow \text{Ar}^{+}(^2\text{P}) + \text{Ar}^{+}(3s^2 3p^4 n1)$ . Detailed measurements show  $n1$  to be  $3d$  and  $4p$  at  $E = 2.4$  keV. The present results are interpreted using the Wigner spin rule and the single electron capture involves a one electron process where the incident  $\text{Ar}^{2+}$  provides the core structure for the outgoing  $\text{Ar}^{+}$  ion. The differential cross sections obtained suggest that single electron capture at small angles involves a strongly attractive intermediate state which couples the incident to the final channels.

Weak exothermic processes are found and in the present study are attributed primarily to highly excited and long lived  $\text{Ar}^{2+}$  states. Although such states constitute an almost negligible fraction of the  $\text{Ar}^{2+}$  they can have very large cross sections for electron capture and result in final  $\text{Ar}^{+*}$  states lying more than 20 eV above the ground state.

The direct scattering in  $\text{Ar}^{2+} + \text{Ar}$  occurs with no Ar target excitation in the  $\tau$  range studied ( $\tau < 3.5$  keV deg). The cross section shows structure primarily due to double electron capture.

References

1. B. Hird and S. P. Ali, J. Phys. B14, 267 (1981).
2. B. A. Huber, J. Phys. B13, 809 (1980).
3. E. Y. Kamber, D. Mathur, and J. B. Hasted, J. Phys. B15, 2051 (1982).
4. J. Aubert, S. Bliman, R. Geller, B. Jacquot, and D. Van Houtte, Phys. Rev. A22, 2403 (1980).
5. R. Johnson and M. A. Biondi, Phys. Rev. A13, 989 (1978).
6. Y. Kaneko, T. Iwai, S. Ohtani, K. Okuno, N. Kobayashi, S. Tsurubac, M. Kimura, and H. Tawara, J. Phys. B14, 881 (1981).
7. K. Okuno and Y. Kaneko, Proc. 12th Internat. Conf. on Physics of Electronic and Atomic Collisions, p. 686 (Gatlinburg, Tenn., 1981).
8. J. Stevens, R. S. Peterson, and E. Pollack, Proc. 12th Internat. Conf. on Physics of Electronic and Atomic Collisions, p. 702 (Gatlinburg, Tenn., 1981).
9. A. Miller, H. Klinger, and E. Salzborn, J. Phys. B9, 291 (1976).
10. V. Sidis, M. Barat, and D. Dhucq, J. Phys. B8, 474 (1975).
11. F. J. Eriksen, S. M. Fernandez, A. V. Bray, and E. Pollack, Phys. Rev. A11, 1239 (1975).
12. S. M. Fernandez, F. J. Eriksen, A. V. Bray and E. Pollack, Phys. Rev. A12, 1252 (1975).
13. A. V. Bray, D. S. Newman, and E. Pollack, Phys. Rev. A15, 2261 (1977).
14. Q. C. Kessel, E. Pollack, and W. W. Smith, in Collisional Spectroscopy, edited by R. G. Cooks (Plenum, New York, 1978), Chap. 3.
15. C. E. Moore, Atomic Energy Levels - NBS circular 467.
16. E. N. Fuls, P. R. Jones, F. P. Ziemba, and E. Everhart, Phys. Rev. 107, 704 (1957).
17. S. W. Nagy, S. M. Fernandez, and E. Pollack, Phys. Rev. A3, 280 (1971).
18. E. W. Rothe and R. B. Bernstein, J. Chem. Phys. 31, 1619 (1959).
19. E. Pollack, E. J. Robinson, and B. Bederson, Phys. Rev. 134, A1210 (1964); R. W. Molof, H. L. Schwartz, T. M. Miller, and B. Bederson, Phys. Rev. A10, 1131 (1974).
20. Y. Hahn, private communication.

Publication

J. Stevens, R. S. Peterson, and E. Pollack. "Electron Capture in Small-Angle  $\text{Ar}^{2+} + \text{Ar}$  Collisions." To be submitted to Phys. Rev. A.

Papers Contributed to Conferences and Meetings

Stevens, J., R. S. Peterson, and E. Pollack. Small-angle  $\text{Ar}^{++} + \text{Ar}$  collisions. Proc. 12th Internat. Conf. on Physics of Electrons and Atomic Collisions, p. 702 (1981).

Pollack, E. and J. Stevens. The Role of Excited State Polarizabilities in Inelastic Collisions. Bull. Am. Phys. Soc. 26:797 (1981).

Stevens, J., T. M. Bastow, L. Pollack, and E. Pollack. Small Angle  $\text{Ar}^{++} + \text{N}_2$  Collisions. Bull. Am. Phys. Soc. 26:1312 (1981).

Degree to be awarded to recipient of ARO support -

Ph.D. to J. Stevens.

Participating Scientific Personnel

Dr. E. Pollack - Professor of Physics  
J. Stevens - Graduate Assistant